

3.1 Theories of woven fabric structure

3.1.1 Introduction

The geometry of fabrics has considerable effects on their behaviour. For example, the weft dimension decreases and weft crimp increases when the cloth is stretched in the warp direction; cloth shrinks when the fibres swell on wetting. Therefore, studies of fabric geometry have played an important role in the following areas:

- (1) prediction of the maximum sett of fabric which should be woven, and fabric dimensional properties;
- (2) derivation of relationship between geometrical parameters, such as crimp and weave angle;
- (3) prediction of mechanical properties by combining fabric geometry with yarn properties such as Young's modulus, bending rigidity and torsional rigidity;
- (4) help in understanding fabric performance, such as in handle and surface effects.

3.1.2 Geometry theories

3.1.2.1 *Yarn configuration in plain-weave fabrics*

As we know, fabrics are not regular structures capable of description in mathematical forms based on geometry; but many believe that we can idealise the general characters of the materials into simple geometrical forms and physical parameters in order to arrive at mathematical deductions. To represent the configuration of threads in woven fabrics, many different forms of geometry have been put forward by textile researchers.

In conventional approaches, the general character of fabrics was idealised into simple geometrical forms. These studies were often based on the

assumption of arbitrary geometrical models for the weave crimp and yarn cross-sectional shapes. They treated the micromechanics of fabrics on the basis of the unit-cell approach, i.e. fabrics are considered as a repeating network of identical unit cells in the form of crimp waves and constant yarn cross-section in the woven structure. By combining this kind of geometry with or without physical parameters, mathematical deductions could be obtained. The yarn configuration in fabric is mainly determined by the form of crimp waves and the cross-sectional shape of yarns in a given position. The cross-sectional shape of yarns in four existing models is reviewed below.

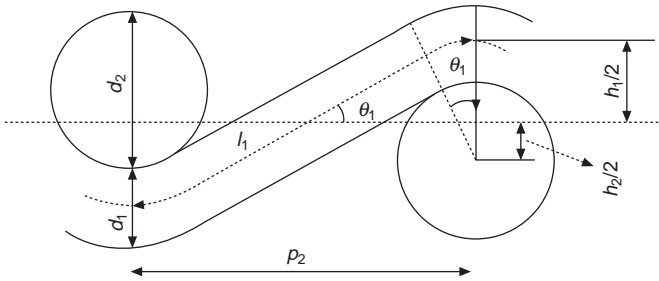
For convenience, the symbols used throughout are listed as follows:

- d – free circular-thread diameter
- D – sum of circular diameters ($d_1 + d_2$)
- a – major diameter of flattened thread
- b – minor diameter of flattened thread
- e – thread flattening coefficient (a/b)
- h – height of crimp wave
- T – fabric thickness ($h_1 + b_1$ or $h_2 + b_2$, whichever is greater)
- p – average thread spacing for the fabric as a whole
- n – average number of threads per unit length ($n = 1/p$)
- c – thread crimp
- K – cover factor
- θ – maximum angle of the thread axis to plane of cloth in radius
- l – length of thread axis between planes containing the axes of consecutive cross threads
- l_c – contact length of yarn
- N – cotton count of yarn

Subscripts 1 and 2 are used to denote warp and weft. If in any relation no subscript is used it is to be understood that either 1 or 2 may be inserted throughout.

The systematic study of woven fabric geometry was started in 1937 when Peirce's paper (Peirce, 1937) was published. Notable examples of geometrical models include Peirce's model of plain-weave fabrics (Peirce, 1937) as shown in Fig. 3.1.

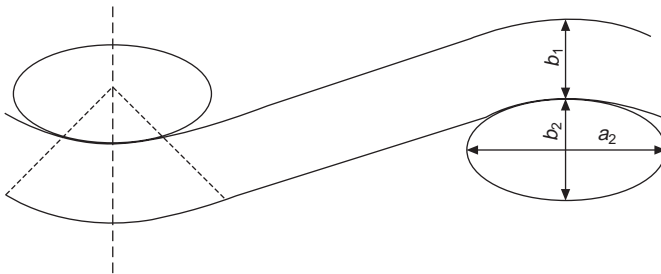
In this model, a two-dimensional unit cell (or repeat) of fabric was built up by superimposing linear and circular yarn segments to produce the desired shape. His model of plain-weave fabrics could be obtained if the yarns were assumed to be circular in cross-section and highly incompressible, but at the same time perfectly flexible so that each set of yarns had a uniform curvature imposed upon it by the circular cross-sectional shape of the interlacing yarns. Derivation of the relationships between the geometrical parameters and such parameters as thread-spacing, weave crimp, weave angle and fabric thickness forms the basis of the analysis. This model is convenient for calculation, and



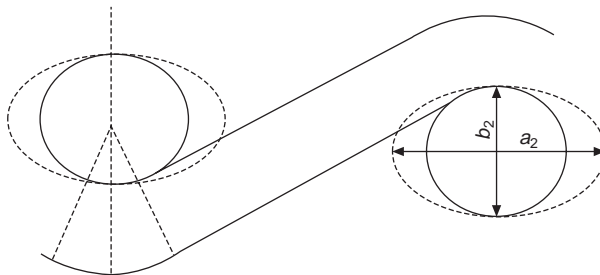
3.1 Peirce's circular cross-section geometry of plain-weave fabrics.

has been found useful in the ordering and interpretation of observation; it is especially valid in very open structures. But the assumptions of circular cross-section, uniform structure along the longitudinal direction, perfect flexibility, and incompressibility are all unrealistic, which leads to the limitations on the application of this model.

In more tightly woven fabrics, however, the inter-thread pressures set up during weaving cause considerable thread flattening normal to the plane of the cloth. Peirce recognised this and proposed an elliptic section theory as shown in Fig. 3.2. Because such geometry would be too complex and laborious in operation, he adopted an approximate treatment, which involved merely replacing the circular thread diameter in his circular-thread geometry with the minor diameter of the appropriate elliptic section as shown in Fig. 3.3.

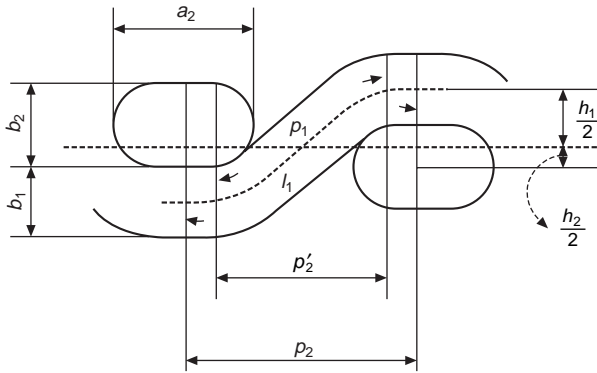


3.2 Peirce's elliptic cross-section geometry of plain-weave fabrics.

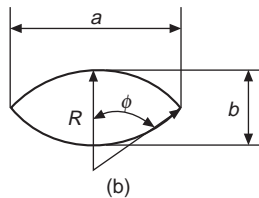
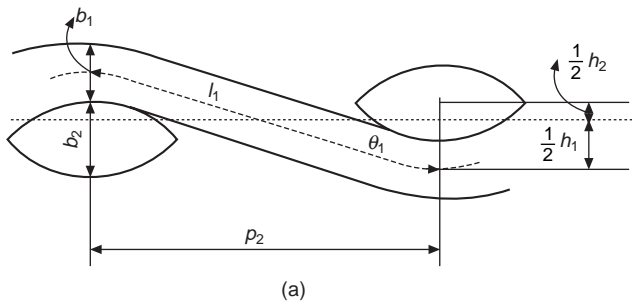


3.3 Peirce's approximate treatment of flattened yarn geometry of plain-weave fabrics.

This treatment was adequate for reasonably open fabrics, but it still does not permit of application to jammed structure. To overcome this difficulty, Kemp (1958) proposed a racetrack section as shown in Fig. 3.4 to modify cross-sectional shape; this consisted of a rectangle enclosed by two semi-circular ends and had the considerable advantage that it allowed the relatively simple relations of circular-thread geometry, already worked out and tabulated by Peirce, to be applied to a comprehensive treatment of flattened threads. In the paper on ‘An energy method for calculations in fabric mechanics’, a lenticular geometry was proposed by Hearle and Shanahan (1978) as shown in Fig. 3.5.



3.4 Kemp's racetrack section geometry of plain-weave fabrics.



3.5 Hearle's lenticular section geometry of plain-weave fabrics.

3.1.2.2 Mathematical description of the models

Among the four models mentioned above, it was found by the author that lenticular geometry developed by Hearle *et al.* and illustrated in Fig. 3.5 is the most general model mathematically. We can establish equations for this model and derive equations for other ones.

The equations for lenticular geometry established by Hearle *et al.* are:

$$\left. \begin{aligned}
 p_i &= (l_j - D_j \theta_j) \cos \theta_j + D_j \sin \theta_j \\
 h_{ii} &= (l_i - D_i \theta_i) \sin \theta_i (1 - \cos \theta_i) \\
 D_i &= 2R_j + b_i \\
 a_{ii} &= 2R_j \sin \theta_i \\
 b_{ii} &= 2T_i \cos \theta_i \\
 e_i &= a_i/b_i \\
 \sin \phi_i &= 2e_i / (1 + e_i^2) \\
 h_1 + h_2 &= b_1 + b_2 \\
 l_{cj} &= D_i \theta_i
 \end{aligned} \right\} [3.1]$$

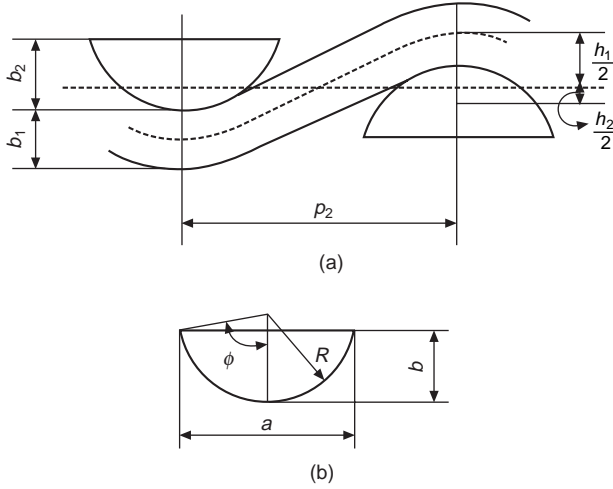
where R_j , is the lenticular radius and θ_i is the lenticular angle.

By substituting $\phi = 90^\circ$, $a_i = b_i = 2R_i = d_i$, $D_1 = D_2 = d_1 + d_2 = D$ into the above equations, the Peirce's geometry as shown in Fig. 3.1 can be obtained. The equations are as follows:

$$\left. \begin{aligned}
 p_1 &= (l_2 - D\theta_2) \cos \theta_2 + D \sin \theta_2 \\
 p_2 &= (l_1 - D\theta_1) \cos \theta_1 + D \sin \theta_1 \\
 h_1 &= (l_1 - D\theta_1) \sin \theta_1 + D(1 - \cos \theta_1) \\
 h_2 &= (l_2 - D\theta_2) \sin \theta_2 + D(1 - \cos \theta_2) \\
 h_1 + h_2 &= d_1 + d_2 = D \\
 l_{c2} &= D_1 \theta_1 \leq l_1 \\
 l_{c1} &= D_2 \theta_2 \leq l_2
 \end{aligned} \right\} [3.2]$$

Therefore, Peirce's geometry can be regarded as a special case of Hearle's lenticular one. And race-track geometry as shown in Fig. 3.4 as a modification of this model, gives the following equations:

$$\left. \begin{aligned}
 p_i &= a_i - b_i + (l'_j - D\theta_j + D \sin \theta_j) \\
 h_i &= (l'_i - D\theta_i) \sin \theta_i + D(1 - \cos \theta_i) \\
 l'_i &= l_i - a_i + b_i \\
 h_1 + h_2 &= b_1 + b_2 = D \\
 l_{cj} &= D_i \theta_i + a_i - b_i \\
 e_i &= a_i/b_i
 \end{aligned} \right\} [3.3]$$



3.6 Bowshaped geometry of plain-weave fabrics.

Including elliptic geometry, the four kinds of geometry are symmetrical ones.

As can be seen in Fig. 3.6, a horizontally asymmetrical geometry which is called bowshaped geometry is also observed frequently. Its geometrical parameters can also be formulated according to the principles of lenticular geometry (Newton and Hu, 1992; Hu and Newton 1993; Hu, 1994) as shown in equation 3.4. The basic equations are identical to those in lenticular geometry except for the two in the square brackets.

$$\left. \begin{aligned}
 p_i &= (l_j - D_j \theta_j) \cos \theta_j + D_j \sin \theta_j \\
 h_i &= (l_i - D_i \theta_i) \sin \theta_i (1 - \cos \theta_i) \\
 D_i &= 2R_i + b_i \\
 a_i &= 2R_i \sin \phi_i \\
 [b_i &= R_i \cos \phi_i] \\
 e_i &= a_i / b_i \\
 [\sin \phi_i &= 4e_i / (4 + e_i^2)] \\
 h_1 + h_2 &= b_1 + b_2 \\
 l_{cj} &= D_i \theta_i
 \end{aligned} \right\} [3.4]$$

3.2 Structural parameters of woven fabrics

From the previous research on the geometric theories introduced above, several parameters could be extracted to characterise the fabric geometry. In this section, a general description of every parameter will be given. Some of them need not be calculated but can only be measured.

3.2.1 Yarn diameter

According to the Peirce's (1937) circular yarn section, $1/d$, and the number of diameters per inch in the cotton system:

$$\frac{1}{d} = \frac{29 \cdot 3\sqrt{N}}{v} \quad [3.5]$$

$$\frac{1}{d} = 28\sqrt{N} \quad [3.6]$$

and

$$d = \frac{1}{28\sqrt{N}} = \frac{0.0357}{\sqrt{N}} \text{ (inch)} = \frac{36}{\sqrt{N}} \text{ (mils)} = \frac{0.91}{\sqrt{N}} \text{ (mm)} \quad [3.7]$$

where v , the specific volume, is the ratio of the volume occupied by a material to that of the same weight of water under compression. Of the woven structure, $v = 1.1$ for cotton yarn.

3.2.2 Thickness

Fabric thickness is given by t_1 or t_2 whichever is greater, where $t_1 = h_1 + d_1$, $t_2 = h_2 + d_2$. When yarn diameters are assumed to be circular:

$$t = \max(t_1, t_2) \quad [3.8]$$

For flattening section yarns, fabric thickness

$$t_1 = h_1 + b_1 \quad t_2 = h_2 + b_2 \quad [3.9]$$

The condition that the two threads project equally produces a smooth surface and gives the minimum thickness, t_{\min}

$$t_{\min} = h_1 + d_1 = h_2 + d_2 = \frac{1}{2}(h_1 + h_2 + d_1 + d_2) = D \quad [3.10]$$

where $h_1 = D - d_1$. So the minimum thickness is the sum of the thread diameters.

The maximum thickness is attained when one or other of the threads is straightened as far as possible. In an open cloth, where either may be straightened to zero crimp, this thickness should be

$$t_{\max} = D + d_{\max} \quad [3.11]$$

d_{\max} is the diameter of the thicker thread, and it is attained by straightening the thinner threads. If $d_1 = d_2 = d$:

$$\begin{aligned} t_{\min} &= 2d = D \\ t_{\max} &= 3d \end{aligned} \quad [3.12]$$

3.2.3 Cover factor

Fabric cover is defined by Hamilton (1964) geometrically as the proportion of fabric area covered by actual yarns. In practice, cover factors are normally calculated for warp and weft independently. For example, a fabric having 50 warp threads per centimetre, each 0.01 cm in major diameter, would have a warp cover factor (K_1) of 0.5 or 50 %. In the case of circular section threads, warp and weft cover factors are given by

$$K_1 = n_1 d_1 \quad K_2 = n_2 d_2 \quad [3.13]$$

For flattened threads, warp and cover factors for plain weave are thus given by

$$K_1 = n_1 a_1 \quad K_2 = n_2 a_2 \quad [3.14]$$

And overall cover factor K is calculated from K_1 and K_2 as follows:

$$K = K_1 + K_2 - K_1 K_2 \quad [3.15]$$

The cover factor thus indicates the degree of closing or cover. Increasing the projection of the area covered by threads through using yarn with greater 'ooziness', or by flattening in finishing and more regularity will improve the cover of cloth.

3.2.4 Crimp

Crimp is the percentage of excess of length of the yarn axis over the cloth length:

$$c_1 = \left(\frac{l_1}{p_2} - 1 \right) \times 100 \% \quad c_2 = \left(\frac{l_2}{p_1} - 1 \right) \times 100 \% \quad [3.16]$$

The primary geometrical parameter is the crimp magnitude. It provides a good basis for investigating many complicated phenomena, such as stress-strain relations, hand and creasing. And, in particular, crimp has been used as a fundamental parameter for calculating other geometrical parameters such as crimp height or weave angle which are not easy to measure. Therefore, to study fabric structure or related problems, measuring yarn crimp in fabric is essential. But the actual difficulty in measuring this parameter is not entirely solved or recognised, perhaps, by many researchers.

3.2.5 General problems

In previous research, much effort has been devoted to the geometry of woven fabrics and related problems under the assumption of constant yarn configuration in fabric. For example, since Peirce, the inter-thread pressure

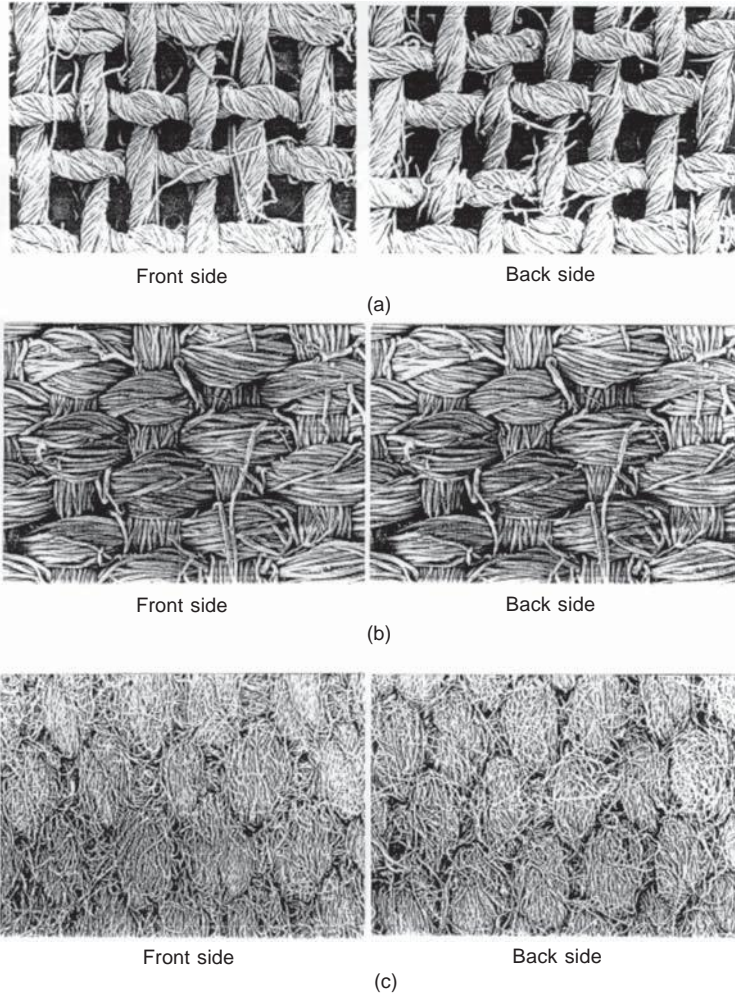
set up during weaving, which causes considerable thread compression, has been recognised as only uniform flattening normal to the fabric plane. His elliptic cross-section model has been regarded as a little bit closer to the actual structure than the circular cross-section due to compressibility. However, the other factors were still not given proper consideration, especially in that it does not permit of any variation along both lateral and longitudinal directions. Adding other models such as Kemp's race-track cross-section and Hearle's lenticular one, the principles on which all these models are based remain unaltered. In particular, it is always assumed either explicitly or implicitly that geometric shape is constant for each model of the unit cell, that is, the variation of the fabric structure was considered insignificant in the analysis. It may not be justified to look only at constant structure and ignore investigation of variation in the structure in the study in fabric geometry.

Firstly, it is a fact that fabrics are extremely complicated materials that do not conform even approximately to any of the ideal features normally assumed in engineering structural analysis and mechanics. Secondly, the measurement of geometrical parameters is not easy in practice. Nobody has measured the full set of geometrical parameters so far, but many rely on the calculations of some formula derived from the geometrical model, mainly from Peirce's model. As we know, there are problems in the model itself. So we have a right to doubt the validity of simplified formulae derived from this model. Therefore, the measurement techniques need to be developed.

Thirdly, a thorough and precise understanding of the effects of fabric geometry on fabric mechanical properties is a precondition for the development of total fabric engineering which will enable a fabric with the right combination of performance characteristics for a particular end use to be designed and manufactured without lengthy and costly trials. But these important effects of fabric construction on fabric mechanical properties tested on the KES system remain almost unexplored.

3.3 Twist redistribution of folded yarns in woven fabrics

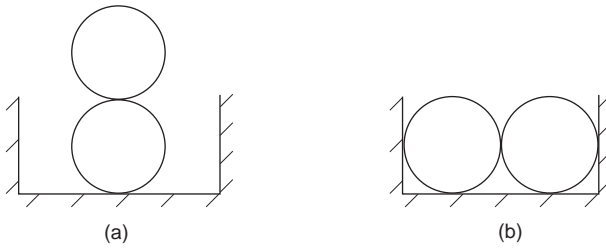
Figure 3.7 shows the surface images of several woven fabrics made of folded yarns. From Fig. 3.7a, which represents a very open woven fabric, it can be seen that the length of a folded yarn in one twist is inserted into one repeat of plain weave fabric. Other samples shown in Figs 3.7b and c exhibit a similar effect. For very close fabrics with few turns of twists, one turn of twist may be inserted into one and a half or two repeats of a plain-weave fabric. There is no literature reporting that a designer would match sett and twists exactly in this way. The phenomenon is here called 'twist redistribution' in a woven fabric because twists of a folded yarn are subjected to adjustment when a woven fabric is formed. It may suggest the contraction of folded



3.7 Surface images of woven fabrics with folded yarns: (a) surface image of an open fabric with folded yarns; (b) surface image of a poplin fabric with folded yarns; (c) surface image of a canvas fabric with folded yarns.

yarns in the longitudinal direction and expansion in the diametrical direction in a woven fabric in most cases. It can be explained in the following ways.

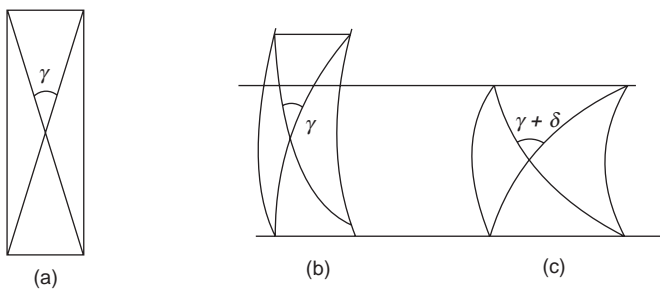
From the above figures, it is also very clear that the two folds of a yarn become parallel with each other and to the fabric plane at the contact region of the two yarn systems of a woven fabric in most cases. This can be explained by the principle of minimum energy when a system reaches an equilibrium state. Figure 3.8 shows a two-cylinder system with the constraints of walls, in which the equilibrium state must be the (b) state.



3.8 Equilibrium condition of two cylinder system.

There may be many states between (a) and (b); whatever the state of the two-cylinder system at the beginning, eventually they will reach the (b) state if there is little friction present. In the case of a folded yarn in a woven fabric, which is constrained by the twists and the adjacent yarns, the parallel state of two folds is enforced by the compression force between warp and weft yarns, and this will increase the twist angle of the folded yarn; thus it contracts the folded yarns per centimetre length of fabric, and the measurement in the diametrical direction will increase if the density of yarns remains the same as that before weaving. Therefore more yarns are contained in 1 cm length of fabric when folded yarns are used. We may think it is similar to the increase of yarn twists.

Figure 3.9 shows the dimensional changes of folded yarns in a certain section of a woven fabric: (a) represents the length of folded yarns before weaving, in which γ is the twist angle of the two folds; (b) represents the length of yarns within a fabric with the assumption that no twist redistribution happens, in which case the twist angle and the width of yarns remain the same as before weaving; (c) describes the actual length of a folded yarn due to the twist redistribution, in which the length of the folded yarn becomes shorter and thicker than before weaving because twist angle γ is increased by σ .



3.9 Dimensional changes of folded yarn in a woven fabric with twist redistribution.

In addition, the twist redistribution might affect the sett of a woven fabric, or make the spacing smaller than designed. But the tested geometrical and mechanical data listed later suggest that while this possibility may exist, it is not very large. In addition, the rule of twist redistribution described above is the general trend; it is not necessarily always exactly true in any segment of yarn because the actual twists may not be exactly matched with the sett even after twist redistribution. This finding, with the other phenomena discussed in other sections, may be useful for understanding the geometrical, mechanical and quality differences between two fabrics, for example two poplin fabrics of which one is made of folded yarns and the other of single yarns, other industrial specifications being similar.

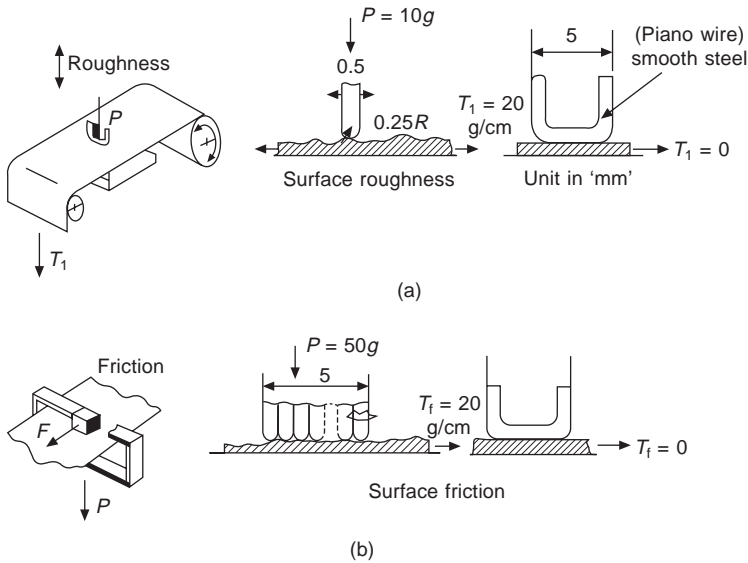
3.4 Relationship between fabric structure and surface properties

3.4.1 Introduction

The properties of a fabric surface are very important in terms of both psychological and physical effects on the human being's appreciation of that fabric. For example, the sensations perceived from the contact of clothing with the skin can greatly influence our overall feeling of comfort. The KES system has a testing machine especially designed for assessing fabric surface properties.

The KES instrument measures the height of a surface of a fabric over a 2 cm length (forwards and backwards) along principal directions. This gives two values for geometrical roughness, *SMD1* and *SMD2*. The geometrical roughness (*SMD*) is a measure of the surface contour of the fabric, an increase in *SMD* suggests an increase in surface variation of a fabric. Figure 3.10 shows the principles of the measurement process.

Interest in studying the geometry of fabric surfaces by objective means goes back to 1955, when Butler *et al.* (1955) reported the design and implementation of their instrument known as the cloth profile recorder. The main objective of the design was the assessment of fabric faults such as repping and the differences in pick spacing along the warp direction. Since this early work, there has been no reported work that describes the objective measurement of surface roughness until the KES system was introduced by Kawabata (1980). Later in 1985, an instrument was introduced which moves the fabric by means of a turnable in order to measure the heights around a 360° rotation. At the same time, a multi-purpose tester was designed by Amirbayat which, in addition to measuring the drape or bending stiffness of fabrics, measures the surface properties and their variation during wear (Hearle and Amirbayat, 1988, Amirbayat and Cooke, 1989). Having realised that there is a force imposed when testing, which affects the measurement of the



3.10 (a) Principles for the measurement of geometrical roughness *SMD*; (b) principles for the measurement of fabric friction coefficient *MIU*.

roughness in the KES surface tester, Ramgulum reported a non-contact method of surface assessment using laser triangulation techniques in 1990 (Ramgulum *et al.*, 1993).

The friction coefficient (*MIU*) is another property measured by the KES surface tester; it is accompanied by its deviation (*MMD*). Kawabata and Mooroka (Barker *et al.*, 1985–1987) separated the coefficient of surface friction into two parts: the first part is associated with the friction between the fabric and the surface of a rigid body. The second component comes from other sources. It is assumed to be related to energy losses caused by inter-fibre friction from compressional deformations occurring when a fabric is subjected to rubbing, denting and crushing. The relative importance of these two terms varies with the type of the surface contact and with the applied load. The deviation of the coefficient of friction (*MMD*) is a measure of slip stick behaviour. The principles involved are shown in Figs 3.10a and b. As the probe sticks and binds on the irregular fabric surface the frictional force changes, giving deviations from the mean friction value.

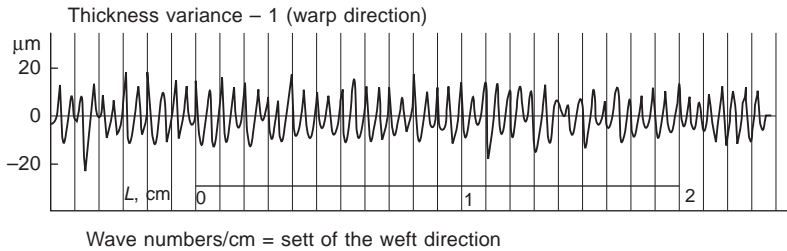
Except for some qualitative explanations as above, existing research on surface properties is generally concerned with the three parameters related with fabric hand or tailorability (Kawabata, 1980; Barker *et al.*, 1985–1987). To the best of the author's knowledge, there exists little investigation of the charts from the KES surface testing and the quantitative relationship between surface properties and fabric geometry.

An investigation will be presented of the characteristics of the geometrical roughness and friction properties of woven fabrics tested by the KES surface tester together with theoretical explanations for these phenomena. A brief discussion will also be provided about the effects of the warp yarn hardening, indicated in Chapter 4, on the surface properties through the comparison of the warp and the weft direction values. Models for the prediction of geometrical roughness and friction properties of woven fabrics will also be developed.

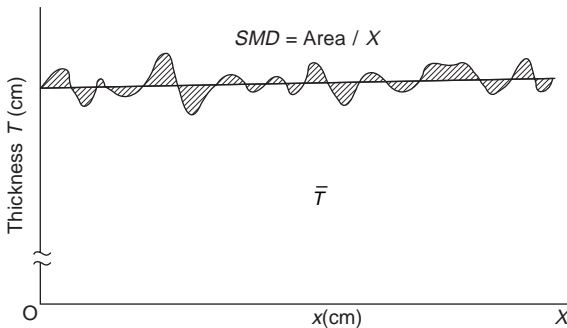
3.4.2 Characteristics of surface geometrical roughness curves

Figure 3.11 is an example of the charts from the KES surface roughness testing. In this figure, the troughs represent the lowest places on the fabric surface, and the peaks the crowns of the yarns in a fabric. The waves on the chart are not very regular, but it was found that the number of the waves generally equals the sett of fabric in the cross direction. The definition of the geometrical roughness in the KES system is included in equation 3.17 and shown in Fig. 3.12.

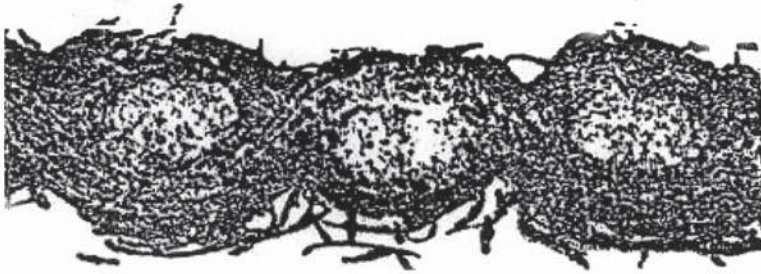
$$SMD = \frac{1}{X} \int_0^x |T - \bar{T}| dx \quad [3.17]$$



3.11 Surface roughness chart measured by the KES system.



3.12 The definition of geometrical roughness (*SMD*).

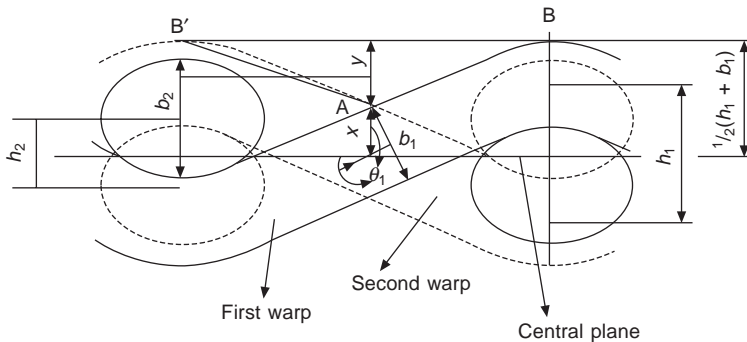


3.13 Cross-section image of plain-weave fabric containing two consecutive yarns.

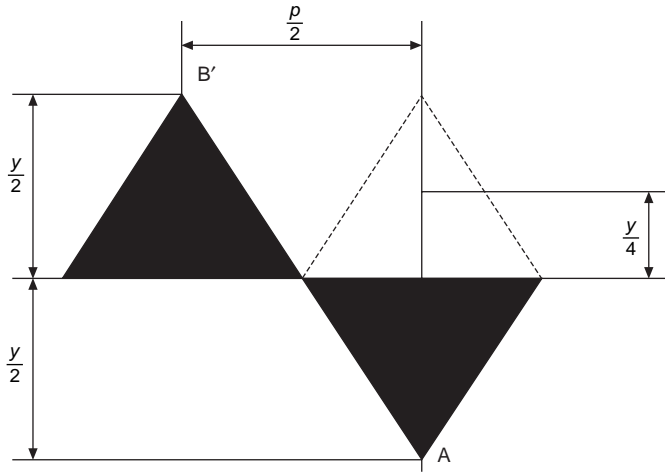
3.4.3 Modelling of fabric geometrical roughness

One of the cross-sectional images of fabric containing two consecutive yarns can be seen from Fig. 3.13. The fabric roughness depends on yarn spacings, irregularity, fabric design and other fabric geometrical factors. If the irregularity of yarns and hairiness are not considered, the geometrical roughness of a woven fabric can be simplified into what is shown in Fig. 3.14, where y is the distance between the lowest places and the highest places on the fabric surface on the tested side. The average thickness of the fabric is located at the centre of y ; the geometrical roughness is a measure of the variation of fabric thickness around the central point of y . From the definition of the KES parameter, *SMD*, it is obvious that the roughness measured is the average height of the area constructed by the average line and the zigzag curves.

If the same principle is used, and the simplified regular roughness change is introduced as in Fig. 3.15, the relationship between fabric roughness and geometrical parameters is as in equations 3.18 and 3.19, where the symbols are the same as in Fig. 3.15; R_t is the theoretical roughness. The average height of the isosceles triangle is:



3.14 Geometrical roughness of woven fabrics.



3.15 Simplified geometrical roughness cycle of woven fabrics.

$$\frac{\frac{1}{2} \left(\frac{1}{2} y \cdot \frac{1}{2} p \right)}{\frac{1}{2} p} = \frac{1}{4} y \quad [3.18]$$

and

$$\begin{aligned} R_{ti} &= \frac{y}{4} = \frac{1}{4} \left(\frac{h_i + b_i}{2} - x \right) = \frac{1}{4} \left(\frac{h_i + b_i}{2} - \frac{b_i}{2 \cos \theta} \right) \quad [3.19] \\ &= \frac{1}{8} \{ h_i + b_i (1 - \cos^{-1} \theta_i) \} \end{aligned}$$

where $i = 1$ and 2 .

3.4.4 Theoretical and measured fabric geometrical roughness

The data obtained from the KES surface testing is called measured roughness to distinguish it from the theoretical roughness as described in equation 3.19. It is found that the theoretical values are always smaller than the measured values and the difference is quite large in some cases. An explanation for this phenomenon is given as follows:

- (1) the simplification of the model is the main reason leading to the smaller calculated values – as can be seen from Figs 3.14 and 3.15, the straight line B'A simply includes a smaller area than the curved line B'A;
- (2) lack of knowledge of the hairiness of yarns and the variation of the fabric structure;

- (3) difficulty in measuring the geometrical parameters may also be responsible for this difference.

3.4.5 Friction properties of woven fabrics

It is interesting to note that, for many fabrics, their friction property charts are closely related to their roughness charts. It can be clearly seen as shown in Fig. 3.16 that they consist of waves, whose number is equal to the sett of the cross-section. Furthermore, the correlation coefficient for the deviation of friction coefficient (*MMD*) and the measured geometrical roughness (*SMD*) is always high. This may suggest that the geometrical roughness contributes to the measured fabric frictional coefficient. We may make use of Fig. 3.14 again to give a description of this relationship.

In Fig. 3.17, we assume the slip stick of the KES surface tester is at different places at different times. B', O', A, O, B are several representative positions. Figure 3.18 is the force analysis which takes the position of O' as an example to derive the relationship between the fabric friction properties and the positions.

The coefficient of the friction between fabric surface and the slip stick is defined as the ratio of the sliding force to the compressional load. The mathematical definition of the *MMD* is as follows:

$$MMD = \frac{1}{X} \int_0^x |\mu - \bar{\mu}| dX \quad [3.20]$$

where X is the testing difference and $\bar{\mu}$ the average function coefficient.

The equilibrium conditions in the x and y axes give the following equations:

$$\left. \begin{aligned} f &= F \cos \alpha + P \sin \alpha \\ N &= P \cos \alpha - F \sin \alpha \end{aligned} \right\} \quad [3.21]$$

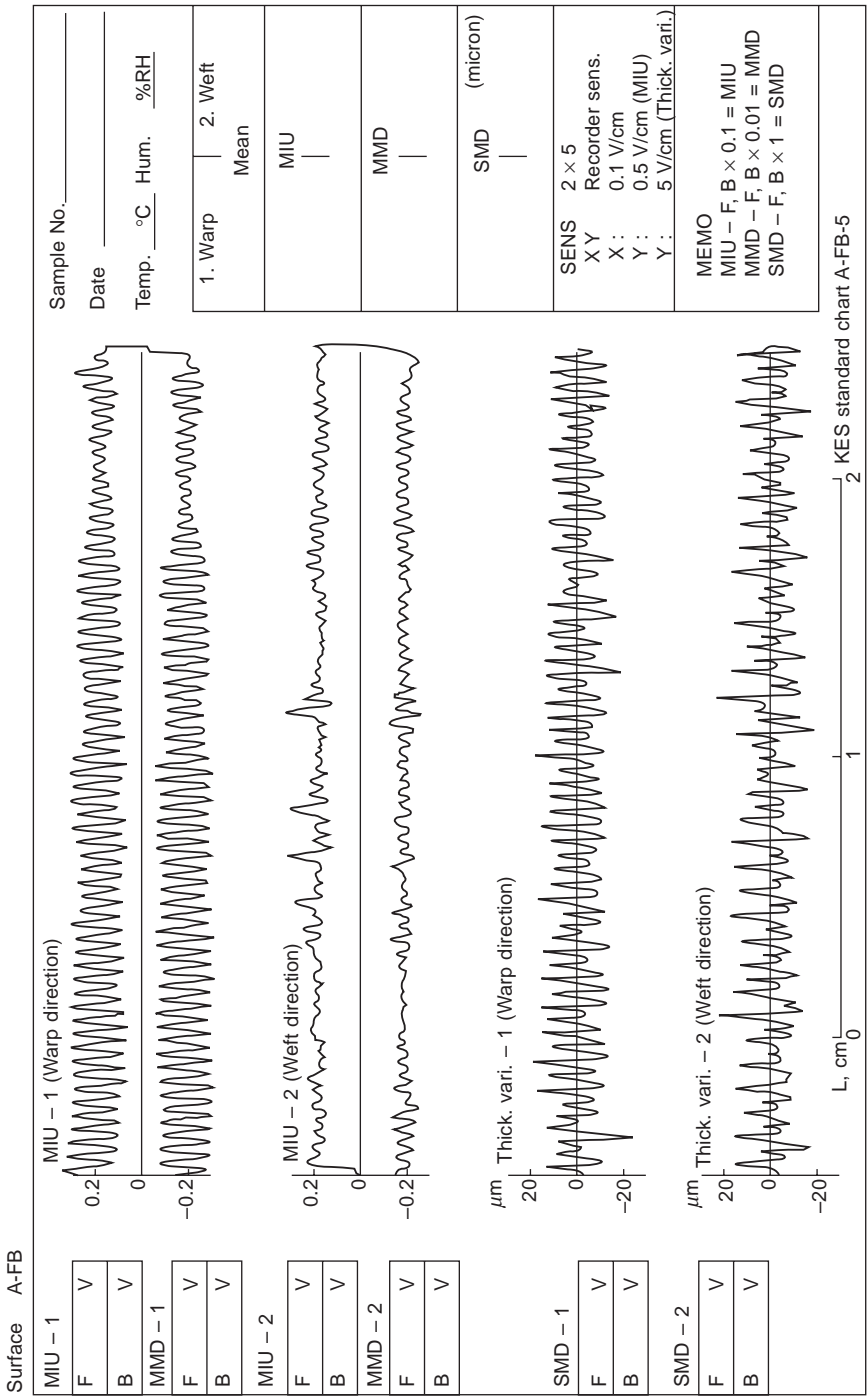
and

$$\mu_y = \frac{f}{N} = \frac{F \cos \alpha + P \sin \alpha}{P \cos \alpha - F \sin \alpha} \quad [3.22]$$

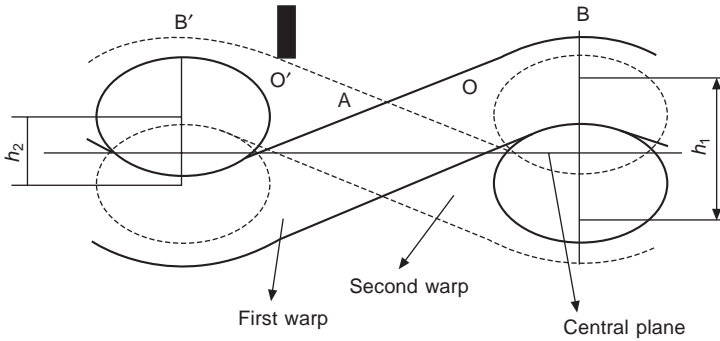
Thus we have

$$\mu_f = \frac{F}{P} = \frac{\mu_y \cos \alpha - \sin \alpha}{\cos \alpha + \mu_y \sin \alpha} = \frac{\mu_y - \operatorname{tg} \alpha}{1 + \mu_y \operatorname{tg} \alpha} \quad [3.23]$$

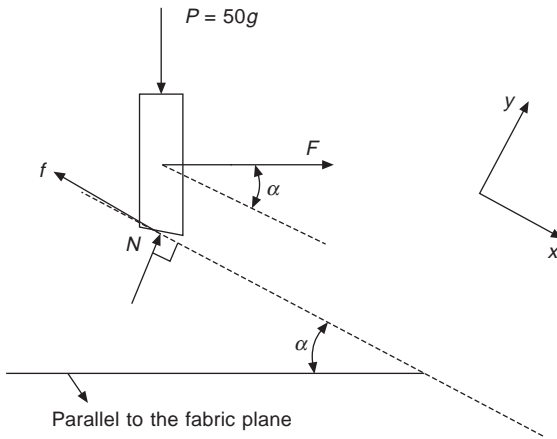
where P is a predetermined constant pressure, F the sliding force along the fabric plane, which can be sensed as friction force in the KES surface tester, N reacting perpendicular to the actual fabric surface, μ_y is the friction coefficient of yarns with the solid stick or the fabric friction coefficient when the



3.16 Comparison of characteristics of friction and surface roughness.



3.17 Positions of friction stick on the fabric surface.



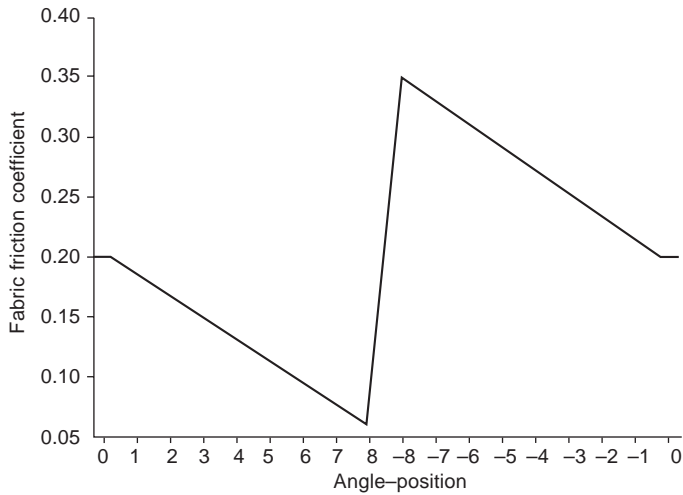
3.18 Force analysis of slip stick.

geometrical roughness is assumed to be zero; and f is the friction force along the actual fabric surface, α the angle of actual fabric surface with the horizontal plane at the position O' in Fig. 3.17. μ_f is the fabric friction coefficient which is equivalent to MIU measured on the KES system. If $\alpha < 0$, the slip stick is in the AOB section, μ_f increases with the increase of $|\alpha|$; if $\alpha > 0$, the stick is in the $B'O'A$ section, μ_f decreases with the increase of α ; if $\alpha = 0$, the stick is at the crown of the yarn wave, the friction coefficient is equal to μ_y ($\mu_f = \mu_y$).

Table 3.1 shows an example of the application of equation 3.23. It is assumed that $\mu_y = 0.2$, the maximum value of α is 8° . From this table we can find that the average fabric friction coefficient μ_f is 0.201448, which is equivalent to definition of MIU measured on the KES system, the deviation of μ_f is 0.073029, which may be regarded as MMD. In addition, Fig. 3.19 indicates that the variation of the friction coefficient is a periodic function. It needs to be noticed that the values of α are very small in this example,

Table 3.1 Predicted friction variation when $\mu_y = 0.2$

Position	α (degree)	α (radian)	μ_f	$\mu_f - \bar{\mu}$
B'	0	0	0.2	0.001448
	1	0.017444	0.181919	0.019529
	2	0.034889	0.163952	0.037496
	3	0.052333	0.146088	0.055360
	4	0.069778	0.128315	0.073133
	5	0.087222	0.110621	0.090827
	6	0.104667	0.092996	0.108452
	7	0.122111	0.075427	0.126021
Both sides of A	8	0.139556	0.057905	0.143543
	-8	-0.139556	0.350310	0.148862
	-7	-0.12211	0.330842	0.129394
	-6	-0.10467	0.311597	0.110149
	-5	-0.08722	0.292561	0.091113
	-4	-0.06978	0.273717	0.072269
	-3	-0.05233	0.255053	0.053605
	-2	-0.03489	0.236554	0.035106
B	-1	-0.01744	0.218208	0.016760
	0	0	0.2	0.001448
Averages			0.201448	0.073029

3.19 Predicted friction variation when $\mu_y = 0.2$.

only 8° . If we increase α , the calculated results are usually larger than the measured ones. Meanwhile, if the average value of μ_y is small, say 0.15, the calculated fabric friction variation tends to be larger than the measured one, as shown in Table 3.2. In a word, the calculated MMD will be far larger than the measured one when the value of MIU is around 0.15 since the usual

values of MMD are generally less than 0.02. In addition, if we increase the value of α , the values of μ_f are even less than zero. Of course this will never be reflected in the actual charts. The reasons for this discrepancy may be caused by the fact that the width of the slip stick is larger (0.5 mm) than we assumed ($< 1/2p = 0.1 \text{ mm} - 0.15 \text{ mm}$), which means that the slip stick need not go through every point as we described in Fig. 3.17.

Table 3.2 Predicted friction variation when $\mu_y = 0.15$

Position	α (degree)	α (radian)	μ_f	$\mu_f - \bar{\mu}$
B'	0	0	0.15	0.001068
	1	0.017444	0.132208	0.018860
	2	0.034889	0.114498	0.036570
	3	0.052333	0.096858	0.054210
	4	0.069778	0.079278	0.071790
	5	0.087222	0.061746	0.089322
	6	0.104667	0.044252	0.106816
Both sides of A	7	0.122111	0.026785	0.124283
	8	0.139556	0.009335	0.141733
	-8	-0.139556	0.296721	0.145653
	-7	-0.122111	0.277836	0.126768
	-6	-0.10467	0.259134	0.108066
	-5	-0.08722	0.240600	0.089532
	-4	-0.06978	0.222221	0.071153
	-3	-0.05233	0.203984	0.052916
	-2	-0.03489	0.185876	0.034808
	-1	-0.01744	0.167886	0.016818
	B	0	0	0.15
Averages			0.151068	0.071746

3.4.6 Comparison between warp and weft surface properties

The comparison between the warp and weft direction surface properties suggests that the warp values of the measured geometrical roughness are likely to be larger than the weft ones; and the warp values of measured friction coefficient, MIU , seem to be smaller than those of the weft ones. This may indicate that the strain hardening of the warp direction affects the surface properties of a woven fabric. It can be explained as follows.

The surface test on the KES system involves a compression load; the work-hardened warp yarns may have higher resistance to compression than the non-hardened weft yarns. Thus, the measured geometrical roughness in the warp direction is likely to be higher than in the weft one. As for the difference in MIU , the plastic strain of warp yarns in the longitudinal direction increases the orientation of fibres in a yarn; thus it reduces the denting and crushing effect when friction occurs.

3.5 Relationship between compression behaviour and fabric structure

The low-load compression behaviour of woven fabrics is very important in terms of hand and comfort. It is also useful for fabric handling during garment manufacturing. In addition, it is found that the analysis of the pressure–thickness relationship may shed light on the structure of fabrics, which may be useful for automatic inspection and image analysis of woven fabrics.

3.5.1 Compression behaviour of fibrous assemblies

Before we deal with fabrics, it is necessary to have a look at the compression behaviour of fibrous assemblies. If a loose sample of wool fibres is compressed, the pressure P exerted on the sample is generally inversely proportional to the cube of the volume v of the sample:

$$P = \frac{\lambda}{v^3} \quad [3.24]$$

where λ is a constant of proportionality (Postle *et al.*, 1988).

Research on the mechanics of the compression of fibre assemblies was initiated by Van Wyk (1946) and reviewed by Carnaby (1980). The compression curve of pressure versus specific volume was derived in his review paper, and the exact relationship describing the compression behaviour of the fibrous mass is

$$P = \lambda \left(\frac{1}{v^3} - \frac{1}{v_0^3} \right) \quad [3.25]$$

where v is the volume of the mass, and v_0 is the value of v when pressure $P = 0$.

In addition to the above relationship for the load–compression of fibrous assemblies, Van Wyk (1946) also suggested a correction to it for assemblies which have been compressed to a volume small enough for the incompressible volume of the fibres to become significant, and for assemblies at zero pressure. The corrected relationship is described in equation 3.26:

$$P = \lambda \left(\frac{1}{(v - v')^3} - \frac{1}{(v_0 - v')^3} \right) \quad [3.26]$$

where v' represents its limiting volume at large pressure. For very loose structure, v' may be negligible and the equation taken the form of equation 3.25.

For over 50 years, this relationship has been examined both experimentally and theoretically for fibrous masses. Despite its shortcomings, Van Wyk's original model has not been superseded. A number of developments have

been reported, which extend its application to assemblies in which the fibres have particular orientations, and finally to fabrics (De Jong *et al.*, 1986; Postle *et al.*, 1988).

3.5.2 Compression behaviour of woven fabrics

3.5.2.1 Application of Van Wyk's law

The process of applying Van Wyk's law to woven fabrics is actually the modelling of pressure–thickness curves. In equation 3.26, if the value of P represents the pressure on a unit area of a fabric, v is equal to the fabric thickness t . With this fact, Postle *et al.* (1988) applied the relationship defined by equation 3.26 and its simplified form to the fabric pressure–thickness curves as a particular case of the fibrous assembly problem.

They began by using the three-parameter equation 3.26 to fit the compression curves of wool fabrics tested on the KES-F compression tester. The fitted curves were in many cases very close to the measured pressure–thickness curves. The incompressible thickness of the fabrics t' is generally between 0.5 and 0.9 of the fabric thickness t at a pressure of 50 gf/cm². They concluded that, in contrast to the application of equation 3.26 to loose wool or silk, the value of t' is not negligible. They also reported that the value of $\lambda(v_0 - v')^3$ in equation 3.26 was small in relation to the maximum pressure $P = 50$ gf/cm² employed in the test. By using this finding and neglecting the last term, they employed a simplified equation:

$$P = \frac{\lambda}{(t - t')^3} \quad [3.27]$$

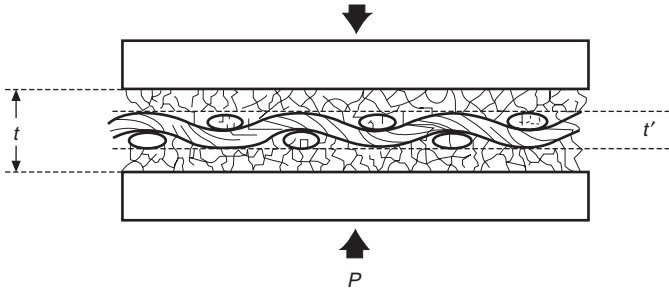
where the thickness t or volume per unit area of fabric is large and undefined at zero pressure.

Furthermore, by utilising the measured thickness T_m of the fabric at a pressure of 50 gf/cm² and the energy WC underneath the pressure–thickness curve between 0.5 and 50 gf/cm²; it was found that the two parameters in equation 3.27 may be calculated:

$$t' = t_m - \frac{2E}{P}, \quad \lambda = \frac{8E^3}{P^2} \quad [3.28]$$

It is assumed that the energy E absorbed by the fabric with the pressure between 0 and 50 gf/cm² equals WC . Thus, on substitution of the measured values of WC for E , and the thickness at 50 gf/cm² for t_m in equation 3.27, the limiting fabric thickness t' and the parameter λ may be determined.

The application of this method to wool fabrics (Postle *et al.*, 1988) showed that the fitted values for λ and t' are in many cases close to the measured KES curves, with some deviation at pressures less than 20 gf/cm². In addition, the measured thickness of a range of fabrics at 1000 gf/cm² and the thickness



3.20 The proposed model of a woven fabric under lateral compression.

extrapolated from equation 3.24, fitted over the range from 0.5–50 gf/cm², correlating well ($r = 0.99$) with slope 1 and an intercept of 0.

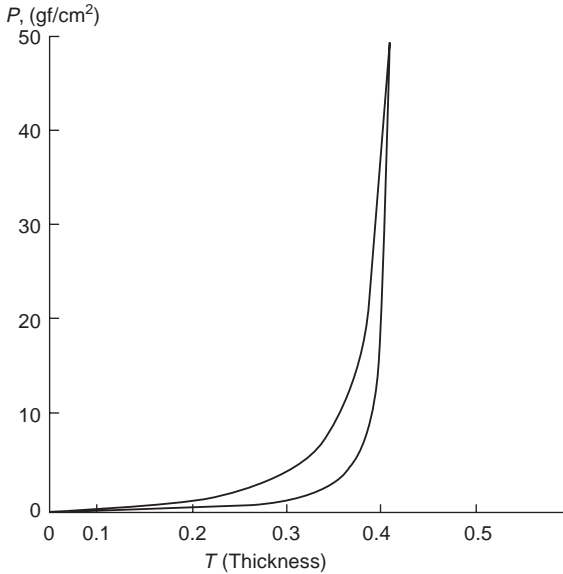
3.5.2.2 Interpretation for fabric structure

de Jong *et al.* (1986) also used equation 3.27 to analyse the mechanics of wool fabric compression in order to interpret the results obtained on wool during finishing. In return, the feedback information could be used for the maintenance of consistent quality in finished fabrics due to the fact that the lateral compression properties of some fabric groups (e.g. wool fabrics) are generally altered by the finishing procedure.

In their analysis, a model, as shown in Fig. 3.20 considers the fabric to consist of three layers: a relatively incompressible core layer in contact with much more compressible surface layers on either side. These two surface layers (the face and back of the fabric) follow Van Wyk's law. As indicated above, the value of λ for these layers is negligibly small. The value of constant t' therefore represents the thickness of the incompressible core of the fabric.

3.5.3 Statement of the problems

Figure 3.21 shows a typical compression curve recorded on the KES system, according to which we may find a close-to-linear relationship between pressure and thickness at the latter part of the curve under a pressure larger than 20 gf/cm². This section of curve is also characterised by a very steep slope which indicates that fabrics are extremely incompressible. Thus the general shape of the curve is largely governed by pressure in the range from 0–20 gf/cm². The values of t_m and WC provided by the KES system are not very reliable for predicting the whole curve because they do not usually match the data read off the curves. Therefore, the universality of the model used by De Jong needs to be proved and its accuracy improved.



3.21 Typical compression (pressure–thickness) curve of woven fabrics.

In the following section, equation 3.27 will be extended to cotton fabrics. As we all know, wool fabric is very different from cotton fabric in structure. As shown in Fig. 3.12, cotton poplin fabrics have very few protruding fibres on their surface while wool fabrics are apparently very hairy. Therefore, although equation 3.27 can be successfully applied to wool fabrics, its applicability to cotton fabrics still awaits confirmation. The method we used is again non-linear regression. Moreover, an alternative method is also introduced to make equation 3.27 easier to use.

In addition, an analysis of equation 3.27 will be given together with a comparison with the measured geometrical thickness. This analysis reveals a clearer picture of fabric structure in which a five-layer structure is suggested.

3.5.4 Fitting of compression curves for cotton fabrics

Inspired by the success of tensile modelling and the comparison of the two kinds of curves (tensile and compression), an attempt was made to use an exponential function to model the pressure–thickness curves. The proposed function is as follows:

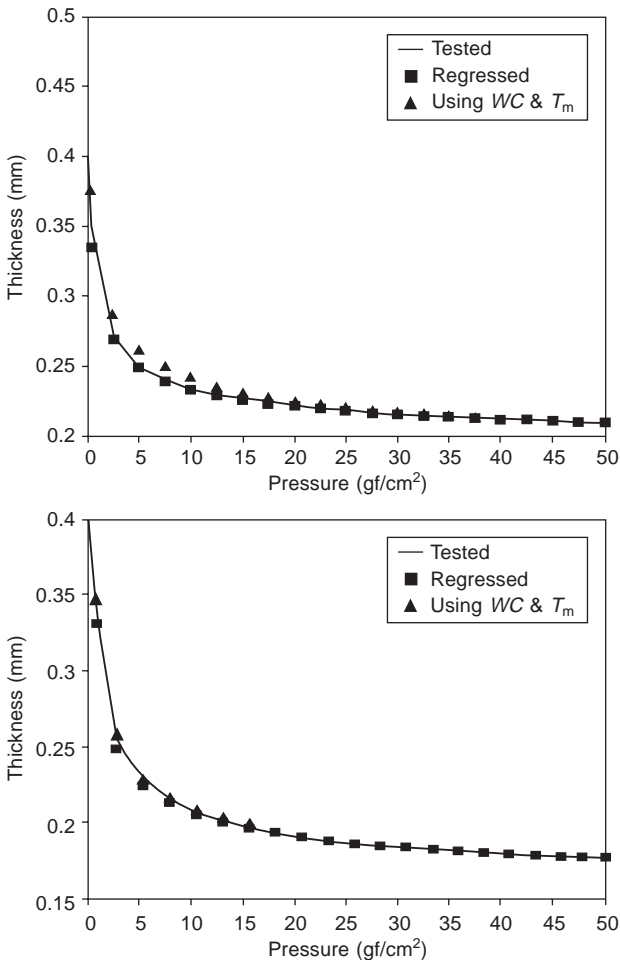
$$P = e^{\alpha t - \beta} - 1 \quad [3.29]$$

where P is pressure and t thickness; two constants α and β need to be estimated.

However, the results fitted by equation 3.29 were not very successful. Therefore, equation 3.27 used by De Jong *et al.* was adopted. We first used two parameters, obtained on the KES system, namely T_m and WC , to fit the

curves. Similar results to wool fabrics can be observed, i.e. good agreement with measured results when the pressure is larger than 20 gf/cm^2 with deviations under pressure less than 20 gf/cm^2 . In other cases, there exist large deviations between the predicted data and the tested results, due to the original deviations of WC and T_m from the data read off the curves or for other unknown reasons.

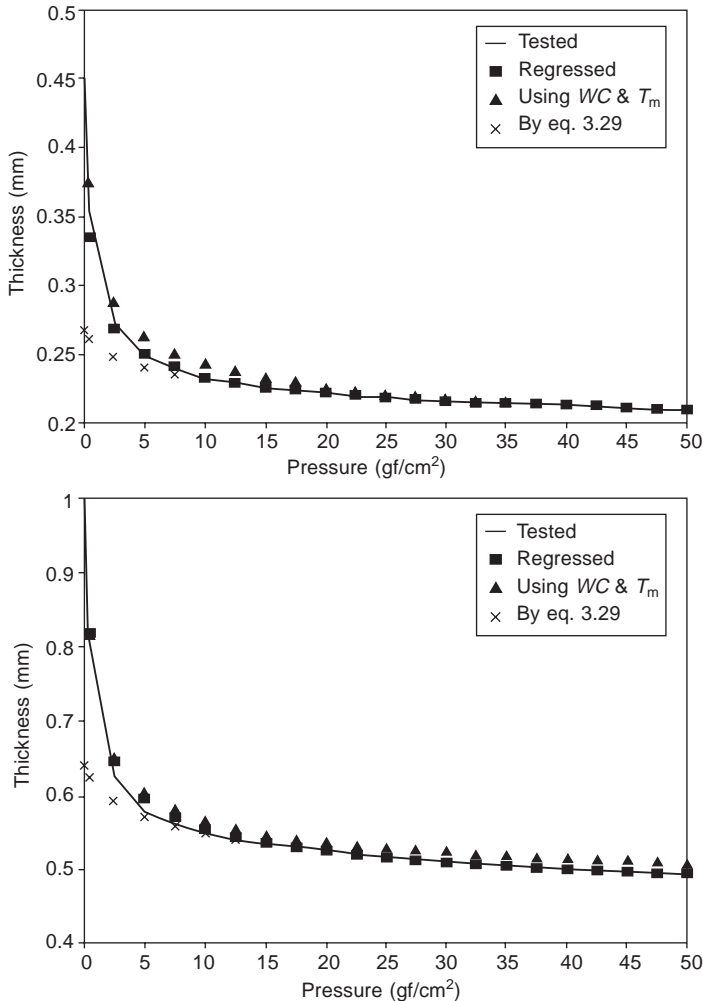
Therefore, a non-linear regression method was employed to improve the goodness of fit of equation 3.27. Three approaches, namely exponential function, power function with two estimations using T_m and WC , and a power function with non-linear regression, are compared. The representative results are shown in Fig. 3.22 together with a comparison of using WC and



3.22 Comparison of compression curve fitted by non-linear regression method and using WC and T_m .

T_m . Sometimes the results fitted using WC and T_m are close to those regressed but, in most cases, the regressed results are much better than those using WC and T_m . Figure 3.23 shows two other examples of comparisons of the results using the three methods, in which cases the results using WC and T_m are comparatively good. However, even here, it is clear that the regression method is more accurate. The residuals or deviations produced by the non-linear regression method are very small, on average only about 1/4 and 1/5 of those produced by using WC and T_m .

From these figures, one can see that the goodness of fit of equation 3.27 to the tested curves may be improved considerably by the non-linear regression



3.23 Comparison of compression curve fitted by three methods.

method. By contrast, the data predicted using WC and T_m demonstrate various degrees of deviation from the tested results.

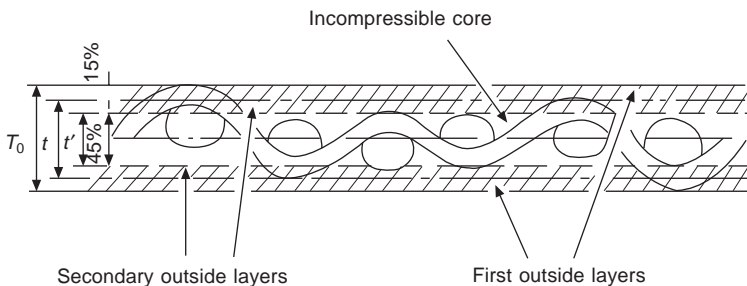
3.5.5 Mechanical and geometrical thickness

According to equations 3.8 and 3.9 above, the fabric thickness with no external pressure, t , may be calculated from the measured geometrical parameters, namely, crimp height h and minor diameter b of yarn. We call this the geometrical thickness. At the same time, one can obtain the fabric thickness from the KES system T_0 , when pressure is at 0.5 gf/cm^2 ; and the thickness T_m when pressure equals 50 gf/cm^2 ; these are called mechanical thicknesses. In addition, from equations 3.8 and 3.9, incompressible thickness t' is also introduced. The comparisons of these thicknesses may be very interesting; in fact, they provide a deeper insight into the fabric structure.

Generally, the geometrical thickness of all woven fabrics lies between T_0 and T_m , or T_0 and t' . The geometrical thickness is actually much smaller than T_0 . This is beyond expectation because the geometrical thickness was measured principally under zero pressure, but T_0 was measured under a pressure of 0.5 gf/cm^2 . Therefore, theoretically, T_0 should be smaller than the geometrical thickness t .

The underlying mechanism for this phenomenon might lie in the fact that during geometrical measurement, crimp height h and minor diameter b were determined by excluding protruding fibres of the yarn surface. Thus the geometrical thickness excludes the hairs on the yarn surface and the crimp crowns above the average thickness. However, the KES compression tester can output everything it can sense, including the hairs and the crimp crowns above the average height of woven fabrics. Therefore, the difference between T_0 and t results from this, and the actual structure of woven fabrics, as shown in Fig. 3.24, is revealed. In it a five-layer structure is still valid but the two outlayers consist of crimp crowns and not only protruding hairs.

In this structure, the furthest outlayers on either side of a fabric contain hairy fibres and crowns above the average geometrical thickness; the secondary



3.24 Five-layer structure of woven fabrics.

layers on either side on a fabric represent another two compressible layers which form the firm structure of the fabric; the t' represents the incompressible core of a fabric. The outlayers and secondary layers of this structure obey Van Wyk's law. The incompressible core layer possesses about 40 % of the whole fabric thickness, which indicates that fabrics are highly incompressible; the two secondary layers have more than 20 %; the first layer about 40 %, which shows that the irregularity of the fabric surface is very large.

3.5.6 Conclusions

Generally speaking, the two-parameter function described by equation 3.27 can quite accurately describe pressure–thickness curves for cotton fabrics provided that the estimation methods are appropriate. It is suggested that the incompressible thickness t' and the parameter λ in equation 3.27 be evaluated or modified by a non-linear regression method. This improves the predictability of the proposed model to a considerable extent. Or, alternatively, in a similar way to what will be described in Chapter 6, they can be evaluated by solving the following two simultaneous equations:

$$\lambda = \sum_{i=1}^n \left(\frac{P_i}{(t_i - t')^4} \right) \cdot \sum_{i=1}^n \left(\frac{1}{(t_i - t')^7} \right) \quad [3.30]$$

and

$$\lambda = \sum_{i=1}^n \left(\frac{P_i}{(t_i - t')^3} \right) \cdot \sum_{i=1}^n \left(\frac{1}{(t_i - t')^6} \right) \quad [3.31]$$

In addition, the relationship between the mechanical and geometrical thickness is found. Comparison of the fabric geometrical and mechanical thickness not only supports the layers theory of fabrics proposed by De Jong, *et al.* but also allows the derivation of a five-layer fabric structure.

3.6 References

- Amirbayat J and Cooke W D (1989), Change in surface properties of fabrics, *Text Res J*, **59**, 469.
- Barker R *et al.* (3/1987, 2/1986, 5/1985), *Reports to North Carolina State University*, Raleigh, North Carolina 27695-8301, Kawabata Consortium, School of Textiles, North Carolina State University.
- Butler K J, Cowhig W T and Michie N A (1955), *Skinner's Silk and Rayon Rec*, **29**, 732.
- Carnaby G (1980), The compression of fibrous assemblies, with applications to yarns and cables, in *Mechanics of Flexible Fibre Assemblies*, Hearle J W S, Thwaites J J and Amirbayat J (eds), Sijthoff and Noordhoff, 99.
- De Jong S, Snath J W and Michie N A (1986), A mechanical model for the lateral compression of woven fabrics, *Text Res J*, **57**, 759.
- Hamilton (1964), A general system of woven fabric geometry, *J Text Inst*, T79.

- Hearle J W S and Amirbayat J (1988), The design of a multipurpose fabric tester, *J Text Inst*, **79**, 588.
- Hearle J W S and Shanahan J W (1978), An energy method for calculations in fabric mechanics, part I: principles of the method, *J Text Inst*, **69**, 81–89.
- Hu J L (1994), *The Structure and Low-stress Mechanics of Woven Fabrics* (PhD thesis, University of Manchester Institute of Science and Technology).
- Hu J L and Newton A (1993), Modelling of tensile stress–strain curves of woven fabrics, *J China Text Univ.*, **10**(4), 49–61.
- Kawabata S (1980), Examination of effect of basic mechanical properties of fabric hand, in *Mechanics of Flexible Fibre Assemblies (NATO Advanced Study Institute Sciences; E, Applied Sciences No. 38)*, Hearle, J W S, Thwaites J J and Amirbayat J (eds), Alpen aan den Rijn, The Netherlands, Sijthoff and Noordhoff, 405.
- Kemp A (1958), An extension of Peirce's cloth geometry to the treatment of nonlinear threads, *J Text Inst*, **49**, T44–48.
- Newton A and Hu J (1992), The geometry of cloth structure, *Proc Inaugural Conference of the Chinese Students and Scholars Textile Association in UK*, Manchester 23.
- Peirce F T (1937), The geometry of cloth structure, *J Text Inst*, **28**, P45–96.
- Postle R, Carnaby G A, and de Jong S (1988), Surface of woven fabrics, in *The Mechanics of Wool Structures*, Poster R, Carnaby G A and de Jang S (Eds), Chichester, Ellis Horwood Ltd, 387.
- Ramgulam R B, Amirbayat J and Porat I (1993), Measurement of fabric roughness by a non-contact method, *J Text Inst*, **84**, 99.
- Van Wyk C M (1946), Note on the compressibility of wool, *J Text Inst*, **37**, T285.